HYDROGEN STORAGE AND MICROSTRUCTURE INVESTIGATIONS OF $La_{0.7-x}Mg_{0.3}Pr_xAl_{0.3}Mn_{0.4}Co_{0.5}Ni_{3.8}$ ALLOYS

G. S. Galdino[1,a], J. C. S. Casini[1], E. A. Ferreira[1], R. N. Faria[1], H. Takiishi[1]
[a]gsgaldino@ipen.br
[1] Department of Metallurgy, Energy and Nuclear Research Institute, IPEN/CNEN-SP, Av. Prof. Lineu Prestes, 2242, ZIP 05508-000, São Paulo, Brazil

Abstract

The effects of substitution of Pr for La in the hydrogen storage capacity and microstructures of $La_{0.7-x}Pr_xMg_{0.3}Al_{0.3}Mn_{0.4}Co_{0.5}Ni_{3.8}$ (x=0, 0.1, 0.3, 0.5, 0.7) alloys electrodes have been studied. X-ray diffraction (XRD), scanning electron microscopy, energy dispersive spectrometry (EDS) and electrical tests were carried out in a the alloys and electrodes. Cycles of charge and discharge have also been carried out in the Ni/MH (Metal hydride) batteries based on the alloys negative electrodes.

Keywords: Praseodymium, metal hydrides, batteries

INTRODUCTION

In the last years, the alloys for the negative electrode material in the second batteries of nickel-metal (Ni/HM) have been incorporating many elements in addition to the basic composition of $LaNi_5$ with the purpose of improving the electrode performance. Environmental safety concerns regarding the toxicity of cadmium and safe disposal of Ni/Cd cells have accelerated the commercialization of Ni/MH cells. (1) Since 1990, large sized Ni-MH batteries (100 Ah) and pure electric vehicles, have been developed by many companies demonstration very high performances for EVs.(2) Praseodymium has been incorporated into the alloys together with mish metal (MM). Pr content varying from 0 to 0.4 at.% in $MMAl_{0.3}Mn_{0.3}Co_{0.4}Ni_{4.0}$ alloys (MM= LaNdPr) has also been reported. The electrode contain with 17 at. %Pr in the MM showed very long cycle life and maximum discharge capacity 370 mAh/g to content similar.(3) Increasing the amount of Ce, Pr and Nd in the alloys led to capacities of 375 mAh/g and better cycling stability.(4) In this study the maximum discharge capacity of various Pr-containing (x= 0-0.7) negative electrodes have been investigated. Hydrogenation at two distinct conditions has been used to determine

the amount of hydrogen absorption in these alloys. Microstructural investigations in these materials have been carried out using a scanning electron microscope.

EXPERIMENTAL

The commercial alloys in the as-cast state and after hydrogenation were studied in this work. The alloys and chemical analysis (showed at Tab. 1) were obtained from the Less Commom Metals Ltda.

Tab.I – Chemical analysis of $La_{0.7-x}Pr_xMg_{0.3}Al_{0.3}Mn_{0.4}Co_{0.5}Ni_{3.8}$ (x = 0 a 0.7) alloys.

Nominal composition (% at)	Composition (% wt)						
	La	Pr	Mg	Al	Mn	Co	Ni
$La_{0.7}Mg_{0.3}Al_{0.3}Mn_{0.4}Co_{0.5}Ni_{3,8}$	25.12	----	1.88	2.09	5.68	7.61	57.62
$La_{0.6}Pr_{0.1}Mg_{0.3}Al_{0.3}Mn_{0.4}Co_{0.5}Ni_{3.8}$	21.52	3.64	1.88	2.09	5.67	7.61	57.59
$La_{0.4}Pr_{0.3}Mg_{0.3}Al_{0.3}Mn_{0.4}Co_{0.5}Ni_{3.8}$	14.33	10.90	1.88	2.09	5.67	7.60	57.53
$La_{0.2}Pr_{0.5}Mg_{0.3}Al_{0.3}Mn_{0.4}Co_{0.5}Ni_{3.8}$	7.16	18.15	1.88	2.09	5.66	7.59	57.47
$Pr_{0.7}Mg_{0.3}Al_{0.3}Mn_{0.4}Co_{0.5}Ni_{3.8}$	----	25.39	1.88	2.08	5.66	7.59	57.41

To hydrogenate five grams of the as cast alloy was exposed to pressure of 200 kPa (2 bar, low pressure) and temperature 773 K and other sample in pressured at 10^3 kPa (10 bar, medium pressure) and room temperature.

In order to prepare the powder to X-ray diffraction and scanning electron microscopy of the following procedure was adopted. The as cast or alloy hydrogenated was crushed with a mortar and pestle in air and such that all the material passed through a < 44 μm sieve. The same method used to characterize the powder was prepared the negative electrode using 140 mg of the powder of the alloy blended with 140 mg of the carbon black (67%) and PTFE (33%). Separator and positive electrode ($Ni(OH)_2$) were taken from a commercial battery. This mixture was manually pressed in a form electrode (~2 cm^2 and 1 mm thick). The electrolyte used was inside the battery (6.0 M KOH solution).

At the charge/discharge cycle tests, charge density adopted in this work was 100 $mAhg^{-1}$ using the current 14 mA during 5 hours and discharge density at 50 $mAhg^{-1}$ discharge at 7 mA until voltage reached -0.9 V.

Samples for the microstructure studies were prepared using conventional metallographic methods. The microstructures of the specimens were examined using a scanning electron microscope with energy dispersive X-ray analysis facility.

RESULTS AND DISCUSSION

Cycle life curves of the negative electrodes prepared using the crushed $La_{0.7-x}Pr_xMg_{0.3}Al_{0.3}Mn_{0.4}Co_{0.5}Ni_{3.8}$ (x = 0 a 0.7) as-cast alloys are shown in Fig. 1.

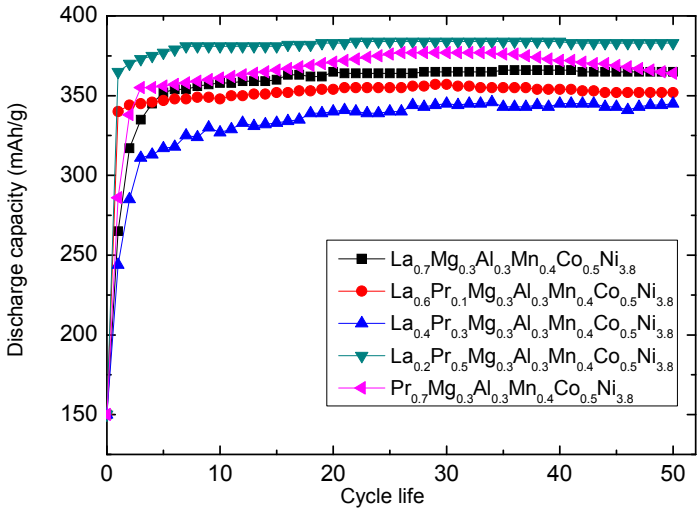

Fig. 1 – Cycle life of negative electrode as-cast alloys.

The substitution of Pr for La decrease discharge capacity until 0.3% at. and total substitution (0.7% at). The best result obtained was $La_{0.2}Pr_{0.5}Mg_{0.3}Al_{0.3}Mn_{0.4}Co_{0.5}Ni_{3.8}$ alloy with a discharge capacity of 384 mAh/g.

Hydrogen absorption data of the $La_{0.7-x}Pr_xMg_{0.3}Al_{0.3}Mn_{0.4}Co_{0.5}Ni_{3.8}$ (x = 0 - 0.7) alloys is given in the Tab.2. The maximum discharge capacity and variation of pressure versus Pr contents in the Fig. 2.

The structure of the $La_{0.7}Mg_{0.3}Al_{0.3}Mn_{0.4}Co_{0.5}Ni_{3.8}$ alloy manually comminuted powder (<44 μm) was showed in the Fig. 3. This same alloy after hydrogenation is shown in the Fig. 4 (a) ~1000 kPa and 293 K and (b) ~200 kPa/ 773 K, respectively.

The $La_{0.2}Pr_{0.5}Mg_{0.3}Al_{0.3}Mn_{0.4}Co_{0.5}Ni_{3.8}$ alloy after hydrogenation is showed in the Fig. 5. (a) ~1000 kPa and 293K and (b) ~200 kPa/ 773K.

Tab. 2 – Hydrogenation of $La_{0.7-x}Pr_xMg_{0.3}Al_{0.3}Mn_{0.4}Co_{0.5}Ni_{3.8}$ (x = 0 a 0.7) alloys for 60 minutes.

X	Medium Pressure			Low Pressure		
	initial (kPa) 293K	final (kPa) 293K	ΔP (P_I-P_F)	initial (kPa) 773K	final (kPa) 773K	ΔP (P_I-P_F)
0.0	1,006	694	394	204	48	156
0.1	1,016	748	268	204	65	139
0.3	1,022	762	260	208	78	130
0.5	1,005	779	226	210	129	81
0.7	1,008	890	118	221	176	45

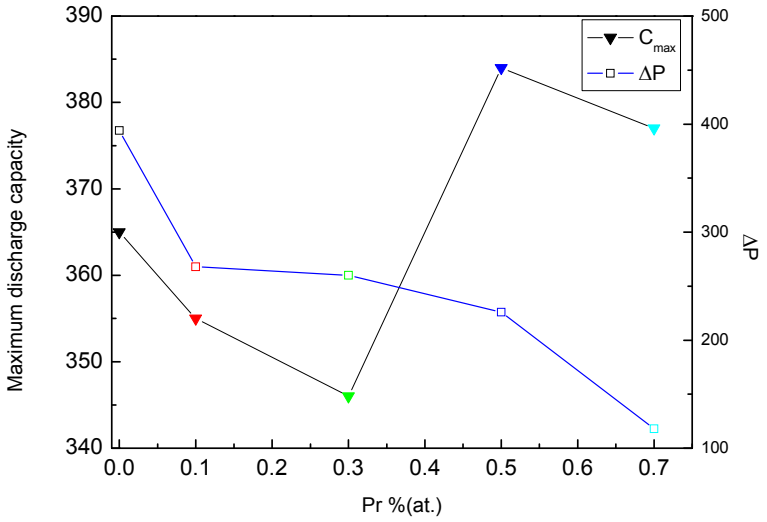

Fig. 2 – Discharge capacity versus praseodymium contents and variation of the pressure.

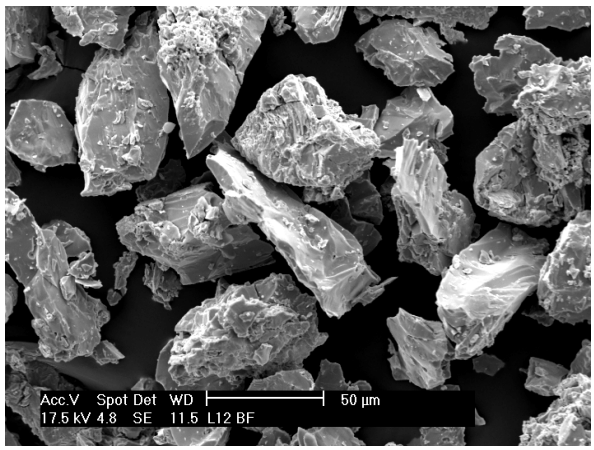

Fig.3 – SEM images of the as-cast $La_{0.7}Mg_{0.3}Al_{0.3}Mn_{0.4}Co_{0.5}Ni_{3.8}$ alloy.

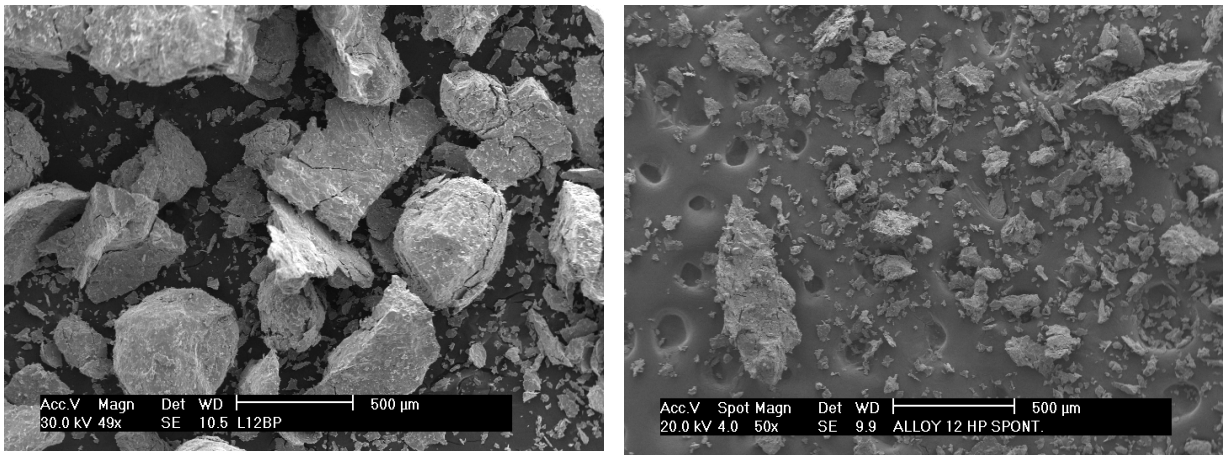

(a) (b)

Fig.4 – SEM images of the hydrogenated $La_{0.7}Mg_{0.3}Al_{0.3}Mn_{0.4}Co_{0.5}Ni_{3.8}$ alloy: (a) in low pressure and (b) in medium pressure.

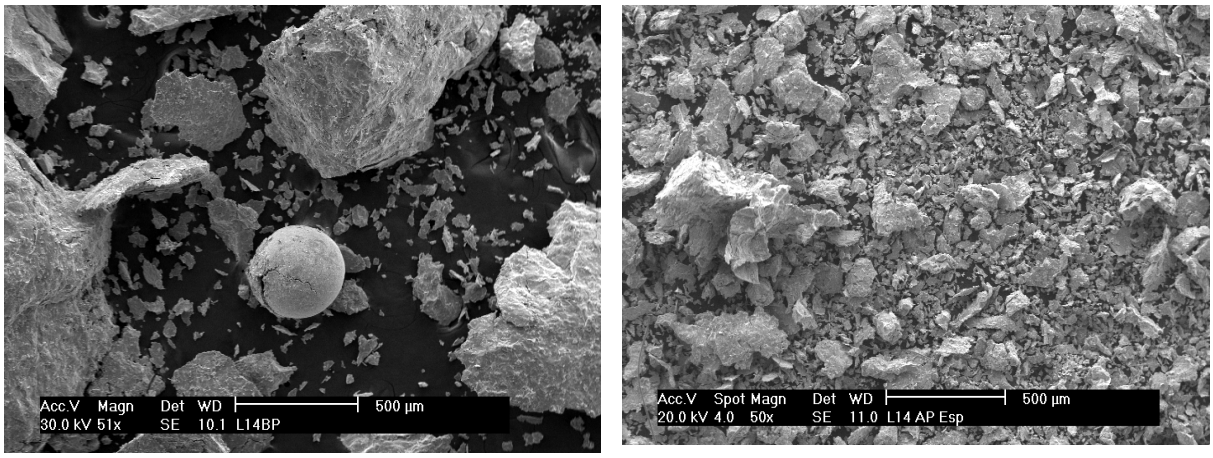

(a) (b)

Fig. 5 – SEM images of the hydrogenated $La_{0.2}Pr_{0.5}Mg_{0.3}Al_{0.3}Mn_{0.4}Co_{0.5}Ni_{3.8}$ alloy: (a) in low pressure and (b) in medium pressure.

Increasing the amount of praseodymium in the alloys decreased the absorption of H_2 for low and medium pressure (Tab. 2). As the Pr-content in the alloys was increased the manual crushing of the hydrogenated alloys became more difficult (to reduce the material to <44 μm).

Backscattered electron micrographic showing a general view and details of the $La_{0.2}Pr_{0.5}Mg_{0.3}Al_{0.3}Mn_{0.4}Co_{0.5}Ni_{3.8}$ as-cast alloy is shown in Fig. 6. This alloy is composed of three phases: the matrix phase (M) and a gray phase (G) and dark gray phase (DG).[5,6] The composition of these three phases in the alloy is given in Tab. 3.

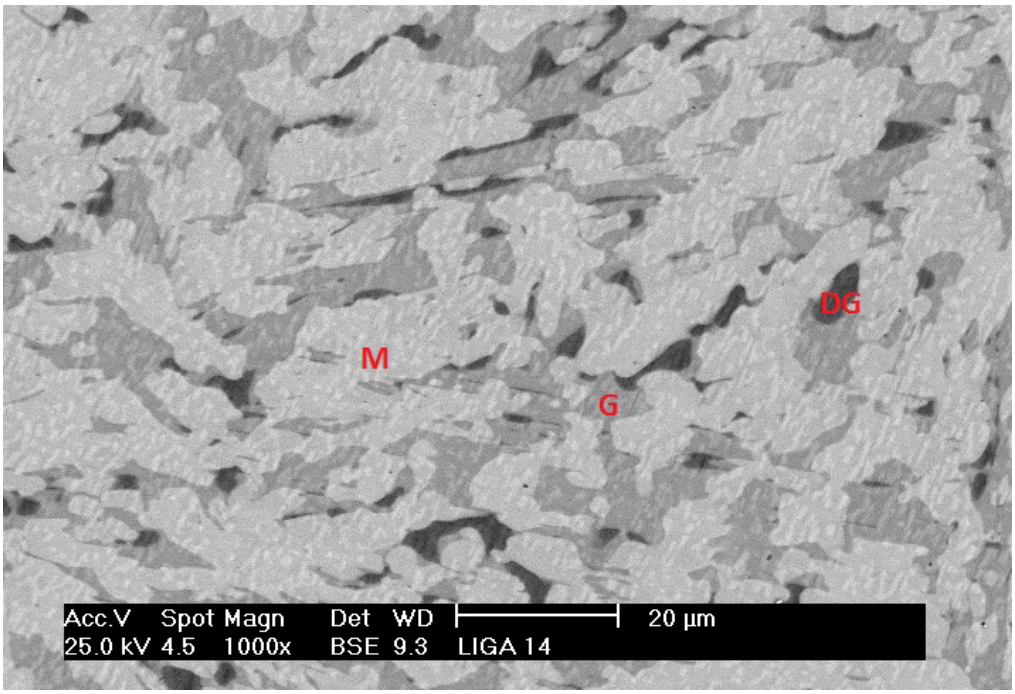

Fig. 6 – Backscattered electron micrograph of the $La_{0.2}Pr_{0.5}Mg_{0.3}Al_{0.3}Mn_{0.4}Co_{0.5}Ni_{3.8}$ alloy.

Tab. 3 – Composition determined by EDX of the $La_{0.2}Pr_{0.5}Mg_{0.3}Al_{0.3}Mn_{0.4}Co_{0.5}Ni_{3.8}$ alloy of the dark gray phase (DG), gray phase (G) and matrix phase (M).

Element / Phase	La	Pr	Mg	Al	Mn	Co	Ni
DG	<1	<1	<1	16.5±0.3	20.2±0.2	14.0±0.4	49.2±0.5
G	2.7±0.3	8.1±0.4	8.1±0.3	2.6±0.2	6.9±0.4	8.0±0.1	63.6±0.3
M	4.2±0.3	11.3±0.2	<1	3.8±0.3	5.0±0.4	8.9±0.3	66.8±0.2

X-ray diffraction patterns of this alloy in the as cast state is shown in Fig. 7. They were identified with M $(La,Pr)Ni_5$ (Space group: P6/mmm – PDF: 50-0777), G $(La,Pr)Mg_2Ni_9$ (Space group: R3m – PDF: 50-1454) and DG AlMnCoNi ($AlMnNi_2$ Space group: Fm-3m – PDF: 65-380). The phase G is important for Ni-MH batteries due high hydrogen storage capacity and good electrode properties. [7,8]

For illustration the X-ray diffraction pattern of the as-cast and hydrogenated $La_{0.7}Mg_{0.3}Al_{0.3}Mn_{0.4}Co_{0.5}Ni_{3.8}$ alloy is shown in Fig. 8. Variations in the 2θ angle for theses alloys in the hydrogenated condition was negligible (≤0.3°).

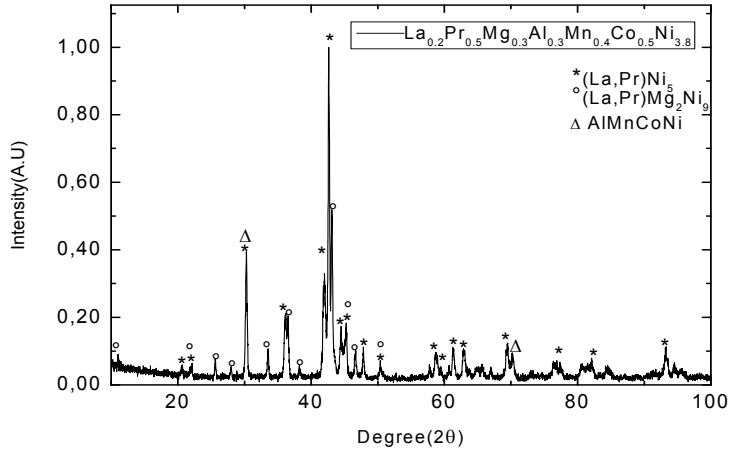

Fig. 7 – XRD patterns for the as cast $La_{0.2}Pr_{0.5}Mg_{0.3}Al_{0.3}Mn_{0.4}Co_{0.5}Ni_{3.8}$ alloy.

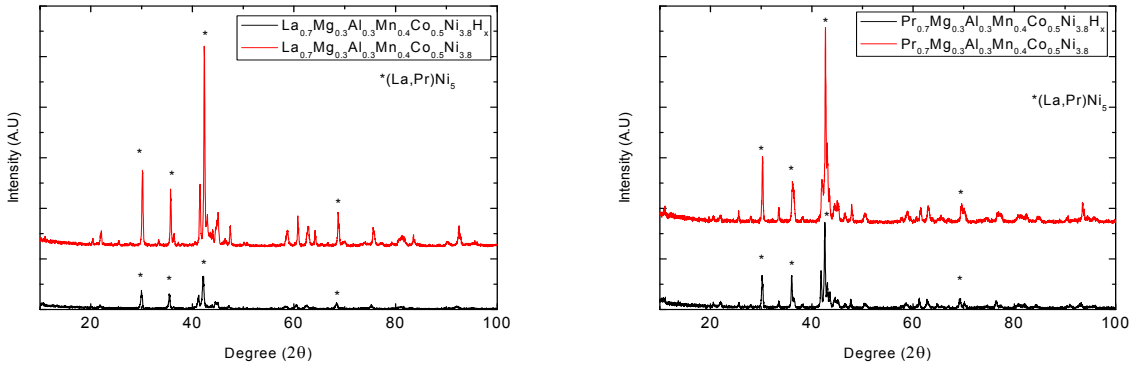

(a) (b)

Fig.8 – XRD patterns for the as cast and hydrogenated a) $La_{0.7}Mg_{0.3}Al_{0.3}Mn_{0.4}Co_{0.5}Ni_{3.8}$ and b) $Pr_{0.7}Mg_{0.3}Al_{0.3}Mn_{0.4}Co_{0.5}Ni_3$ alloys.

CONCLUSIONS

A negative electrode produced using the $La_{0.2}Pr_{0.5}Mg_{0.3}Al_{0.3}Mn_{0.4}Co_{0.5}Ni_{3.8}$ cast alloy exhibited a maximum discharge capacity of 384 mAh/g. Medium hydrogenation pressure was more effective than that performed at low pressure. Increasing the praseodymium content in the alloys led to brittle alloys.

ACKNOWLEDGEMENTS

The authors thank the National Council for Scientific and Technological Development (CNPq), The State of São Paulo Resource Foundation (FAPESP) and the Energy and Nuclear Research Institute (IPEN) for the financial support and

infrastructure which made available this investigation. The authors are also indebted to E.P. Soares for the micrographys of the hydrogenated alloy. Thanks for Milton Cioffi of Indaco industry LTDA for providing us a sample of PTFE.

REFERENCES

1. F. Feng, M. Geng, D.O. Northwood, Electrochemical behaviour of intermetallic-based metal hydrides used in Ni/metal hydride (MH) batteries: a review. ***Int. Journal of Hydrogen Energy***, Ontario, CA, v.26 p.725–734, 2001.

2. Tetsuo Sakai, Ituki Uehara, Hiroshi Ishikawa, R&D on metal hydride materials and Ni-HM batteries in Japan. ***Journal of Alloys and Compounds***, Osaka, JA, v.293-295, p.762-769, 1999.

3. E.P. Banczek, L.M.C. Zarpelon, R.N. Faria, I. Costa, Corrosion resistance and microstructure characterization of rare-earth-transition metal–aluminum–magnesium alloys. ***Journal of Alloys and Compounds***, São Paulo, BR, v. 479 p. 342-347, 2009.

4. YAN Huizhong, KONG Fanqing, XIONG Wei, LI Baoquan, LI Jin, Effect of praseodymium substitution for lanthanum on structure and properties of $La_{0.65-x}Pr_xNd_{0.12}Mg_{0.23}Ni_{3.4}Al_{0.1}$(x=0.00-0.20) hydrogen storage alloys. ***Journal of Rare Earths***, Baotou, CH, v. 27, p. 244-249, 2009.

5. L.M.C. Zarpelon, E. Galego, H. Takiishi, R.N. Faria, Microstructure and Microanalysis Studies of Some Lanthanum-Magnesium Based Hydrogen Storage Alloys, ***Materials Research***, São Paulo, BR, v.11 p. 17–21, 2008.

6. L. M. C. Zarpelon, E. Galego, H. Takiishi, R. N. Faria, Microstructure and Composition of Rare Earth-Transition Metal-Aluminium-Magnesium Alloys, ***Materials Research***, Vol. 11, No. 1, 17-21, 2008.

7. KADIR, K.; SAKAI, T.; UEHARA, I. Structural investigation and hydrogen capacity of YMg_2Ni_9 and $(Y_{0.5}Ca_{0.5})(MgCa)Ni_9$: new phases in AB_2C_9 system isostructural with $LaMg_2Ni_9$. ***Journal of Alloys and Compounds,*** Osaka, JP, v.287, p. 264-270, 1999.

8. PAN, H.; CHEN, N.; LEI, Y.; WANG, Q. Effects of annealing temperature and the electrochemical properties of $La_{0.7}Mg_{0.3}Al_{0.2}Mn_{0.1}Co_{0.75}Ni_{2.45}$ hydrogen storage alloy. ***Journal of Alloys and Compounds***, Hangzhou, CN, v.397, p. 306-312, 2005.